

## Hydrogen trapping by solute atoms in Nb–Mo(3 at. %) alloys as observed by the channeling method

Eiichi Yagi, Shiho Nakamura,\* Fumihisa Kano,\* and Takane Kobayashi  
*The Institute of Physical and Chemical Research, Wako-shi, Saitama 351-01, Japan*

Kenji Watanabe and Yuh Fukai  
*Department of Physics, Chuo University, Kasuga, Bunkyo-ku, Tokyo 112, Japan*

Takehiko Matsumoto  
*National Research Institute for Metals, Nakameguro, Meguro-ku, Tokyo 153, Japan*  
(Received 3 August 1988)

In order to elucidate the mechanism of the enhancement of the terminal solubility for hydrogen (TSH) in Nb by alloying with undersized Mo atoms, the state of hydrogen was studied by the channeling method using a nuclear reaction  ${}^1\text{H}({}^{11}\text{B}, \alpha)\alpha\alpha$  in Nb–Mo(3 at. %) alloys. At room temperature H atoms are located at sites displaced from tetrahedral (*T*) sites by about 0.6 Å towards the nearest-neighbor lattice points, while at 373 K they are at *T* sites. These results give direct evidence for trapping of hydrogen by Mo atoms and strongly support the trapping model for the enhancement of the TSH in the low-concentration region of Mo atoms.

The effect of alloying on the terminal solubility for hydrogen (TSH) in group Va metals (V, Nb and Ta) has been investigated for various alloying elements.<sup>1–12</sup> It has been reported that for undersized metal solutes, e.g., Nb in Ta and V in Nb, the TSH increases rapidly with metal solute concentration, and for oversized solutes, e.g., Ta in Nb and Nb in V, the TSH again increases with increasing solute concentration but less rapidly.<sup>6</sup> Matsumoto, Sasaki, and Hihara found from x-ray diffraction<sup>1</sup> and NMR studies<sup>3</sup> that the dissolution of hydrogen reduces the existing strain due to undersized solute atoms V and Mo in Nb, and proposed that this is an indication of trapping of hydrogen by these solute atoms. As the stress relaxation is expected to be more efficient as hydrogen comes closer to a solute atom, this in effect gives rise to strong attractive interaction between undersized solute atoms and hydrogen. For oversized substitutional solute atoms, Westlake and Miller suggested that the solutes distend nearby interstitial sites in such a way that certain sites may become more favorable for hydrogen occupancy.<sup>4</sup> In this way, oversized solutes may also lead to hydrogen trapping and subsequently the enhanced TSH. On the other hand, Peterson and co-workers reported that evidence of trapping could not be observed in the studies on the isopiestic solubility of hydrogen and the hydrogen diffusion in V-based alloys (V–Nb, V–Cr, and V–Ti) for a wide range of solute concentration and, therefore, the enhancement of the TSH could not be ascribed to a simple trapping of hydrogen.<sup>10,11</sup> Oates and Flanagan suggested that the enhancement of the TSH on alloying is likely to be fairly general and explained this by considering only the average effect of alloying on macroscopic thermodynamical quantities.<sup>12</sup> Therefore, the mechanism of the enhancement of the TSH is still an open question, and more detailed information is required.

If a strong interaction exists between hydrogen and undersized solutes as described above, it may cause some change in the lattice location of hydrogen. Hence, observation of the lattice location of hydrogen will give information on the nature of this attractive interaction if any and, accordingly, on the mechanism of the enhancement of the TSH. In the present study the lattice location of hydrogen was investigated in the Nb–Mo(3 at. %) alloy by the channeling method utilizing a nuclear reaction  ${}^1\text{H}({}^{11}\text{B}, \alpha)\alpha\alpha$ .<sup>13–15</sup>

Hydrogen was doped from the gas phase up to a concentration of 2 at. % or 5 at. % into Nb–Mo(3 at. %) single-crystal slices about 1 mm thick. These concentrations are within the TSH at room temperature. The channeling angular scan was made with respect to the  $\langle 100 \rangle$  and  $\langle 110 \rangle$  axes and the  $\{100\}$  plane with a 2.03-MeV  ${}^{11}\text{B}^{2+}$  beam under the same condition as described in a previous paper.<sup>15</sup> Results obtained at room temperature are shown in Fig. 1 as a function of incident angle  $\psi$  with respect to the channeling direction. The effect of radiation damage or hydrogen trapping at defects introduced by analysis-beam irradiation on the angular profiles of  $\alpha$ -particle yields ( $\alpha$ -angular profiles) was checked in a way similar to that previously reported.<sup>13</sup> The effect was small, probably because the hydrogen concentration was high in comparison with that of defect traps.

When the concentration of hydrogen is lower than that of Mo [Nb–Mo(3 at. %)–H(2 at. %), Fig. 1(a)], the  $\alpha$ -angular profiles are very different from those for the tetrahedral (*T*) site occupancy observed for the  $\alpha$ -phase of an Nb–H system.<sup>16</sup> In the Nb–H system, the  $\alpha$ -angular profiles exhibited a large central peak at  $\psi=0^\circ$  for the  $\langle 100 \rangle$  channel, a large central peak consisting of three subpeaks at  $\psi=0^\circ$  and  $\sim \pm 0.35^\circ$  for the  $\langle 110 \rangle$  channel, and a small central peak superposed on a shallow dip for

the  $\{100\}$  channel.<sup>16</sup> In the Nb–Mo(3 at.%)–H(2 at.%) alloy, on the other hand, the  $\alpha$ -profiles did not exhibit a peak at  $\psi=0^\circ$  for all three channels, but exhibited a small peak at  $\psi \approx 0.1^\circ$  for the  $\langle 100 \rangle$  channel, as well as much smaller off-center peaks at  $\psi \approx \pm 0.2^\circ$  and  $\sim -0.6^\circ$  for the  $\langle 110 \rangle$  channel, and a shallow dip for the  $\{100\}$  channel. Hence, most of the hydrogen atoms are considered to be located at sites different from  $T$  sites.

When the concentration of hydrogen becomes higher than that of Mo [Nb–Mo(3 at.%)–H(5 at.%)], Fig. 1(b), the  $\alpha$ -angular profiles change markedly. The  $\langle 100 \rangle$   $\alpha$ -angular profile exhibited a higher central peak at  $\psi=0^\circ$ . In the  $\langle 110 \rangle$  channel, much higher subpeaks appeared at  $\psi=0^\circ$  and about  $\pm 0.35^\circ$ , and the small peak around  $-0.6^\circ$  observed in Fig. 1(a) was still present. The  $\{100\}$   $\alpha$ -dip became deeper, and a very small central peak appears to be superposed on the dip. Newly observed subpeaks were located at the same angular positions as observed in the  $\alpha$ -phase of the Nb–H system.<sup>16</sup> These results suggest that some fraction of the H atoms are located at  $T$  sites.

After the measurements at room temperature, the channeling experiments were performed at 373 K on the specimen of Nb–Mo(3 at.%)–H(5 at.%) (Fig. 2). As compared with the results at room temperature, the  $\langle 100 \rangle$   $\alpha$ -angular profile exhibited a much higher central peak at  $\psi=0^\circ$ , and in the  $\{100\}$  channel the central peak

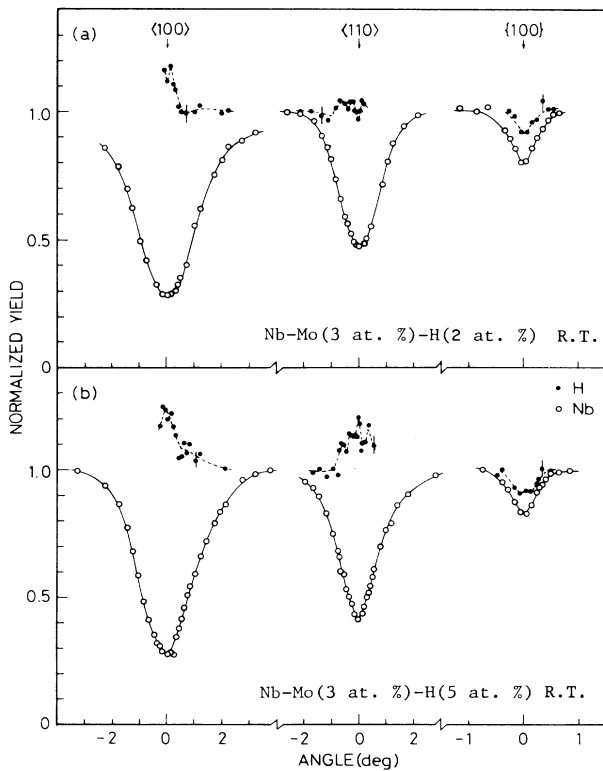


FIG. 1. Channeling angular profiles of  $\alpha$ -particle and back-scattered  $^{11}\text{B}$  yields obtained at room temperature for (a) the Nb–Mo(3 at.%)–H(2 at.%) alloy and (b) the Nb–Mo(3 at.%)–H(5 at.%) alloy. The solid curves and dashed curves have been drawn to guide the eye.

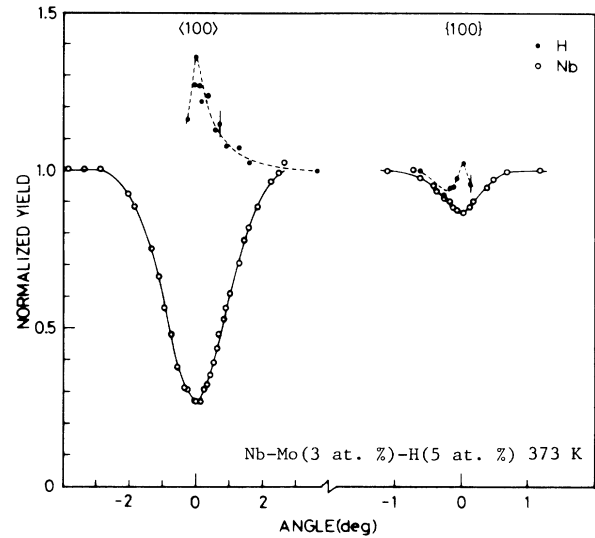


FIG. 2. Channeling angular profiles of  $\alpha$ -particle and back-scattered  $^{11}\text{B}$  yields obtained at 373 K for the Nb–Mo(3 at.%)–H(5 at.%) alloy. The solid curves and dashed curves have been drawn to guide the eye.

superposed on the dip became much more conspicuous. These profiles are characteristic of  $T$ -site occupancy.<sup>16</sup>

The results described above can be interpreted as follows. In the Nb–Mo(3 at.%)–H(2 at.%) alloy most of the H atoms are trapped by Mo atoms and located at sites different from  $T$  sites (trapped sites) at room temperature. In the Nb–Mo(3 at.%)–H(5 at.%) alloy, some fraction of the H atoms are located at trapped sites and the rest are at  $T$  sites at room temperature, while at 373 K, the H atoms are detrapped and enter  $T$  sites.

The lattice location of the trapped site was determined by fitting the calculated angular profiles to the observed profiles. The calculation was made on the basis of a multistring model by using the Erginsoy formula for a continuum potential.<sup>17</sup> In this calculation, lattice vibration and beam divergence were not taken into account, and only a change in the transverse energy of incident ions,  $E_{\perp}$ , due to scattering by electrons, was considered. The average increase in  $E_{\perp}$ ,  $\delta E_{\perp}$ , during penetration to a distance  $\delta Z$  is given by

$$\delta E_{\perp} \approx \frac{m_e}{2M_1} \frac{dE}{dZ} \delta Z, \quad (1)$$

where  $dE/dZ$  is a stopping power, and  $m_e$  and  $M_1$  are the masses of an electron and an incident ion, respectively.<sup>18</sup>  $\delta Z$  was taken to be 60 nm, corresponding to the depth where a nuclear-reaction cross section becomes about one fourth of the value at the resonance peak.  $\delta E_{\perp}$  amounted to 1.8 eV.

The  $\alpha$ -angular profiles were calculated in the five cases shown in Fig. 3, namely, that all H atoms are located at (a) sites displaced from octahedral ( $O$ ) sites by  $d$  in the  $\langle 110 \rangle$  direction, (b) sites displaced from lattice points by  $d$  in the  $\langle 111 \rangle$  direction, (c) sites displaced from  $T$  sites by  $d$  towards the nearest-neighbor lattice points, i.e., in the  $\langle 120 \rangle$  direction, (d) sites displaced from  $T$  sites by  $d$

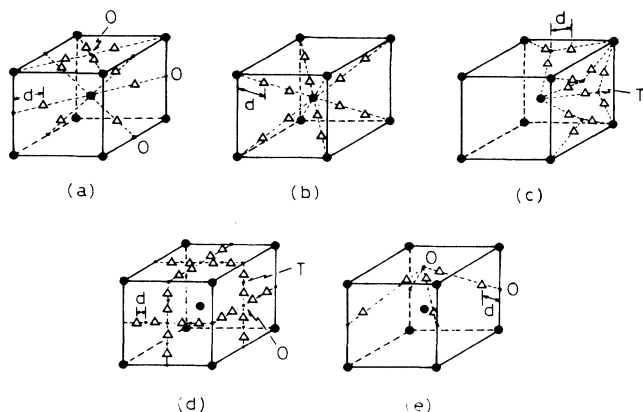


FIG. 3. Various types of lattice location for hydrogen ( $\Delta$ ), for which  $\alpha$ -angular profiles were calculated (Fig. 4). In each type of group only some fraction of equivalent sites are indicated.

towards the nearest-neighbor  $O$  sites, or (e) sites displaced from  $O$  sites by  $d$  in the  $\langle 111 \rangle$  direction. Sites displaced from lattice points in the  $\langle 100 \rangle$  direction, and those displaced from  $O$  sites to the nearest-neighbor lattice points, i.e., in the  $\langle 100 \rangle$  direction, were excluded from this consideration, because a dip expected in the  $\langle 100 \rangle$   $\alpha$ -angular profile due to shadowing of one third of these sites by  $\langle 100 \rangle$  atomic rows was not observed. The magnitude of displacement,  $d$ , was chosen so that the calculated  $\alpha$ -

angular profile reproduces a subpeak observed around  $\psi = -(0.5-0.6)^\circ$  for the  $\langle 110 \rangle$  channel. The observed  $^{11}\text{B}$ -angular profiles showed partially appreciable deviation from the corresponding calculated curves. This deviation was attributed to the increase of a random fraction of an incident  $^{11}\text{B}$  beam due to dechanneling by the lattice disorder in the specimen crystal. The calculated  $\alpha$ -angular profiles were corrected by taking account of such an additional random fraction.

The  $\alpha$ -angular profiles calculated for the Nb-Mo(3 at. %)-H(2 at. %) alloy are shown in Fig. 4. As shown in Fig. 4(f), the observed  $\alpha$ -angular profiles were best fitted by the calculated profiles for the lattice location of hydrogen of type (c) with  $d = 0.62 \text{ \AA}$ , which is about 34% of the distance between a  $T$  site and its nearest-neighbor lattice point. Hence, it is concluded that in the Nb-Mo(3 at. %)-H(2 at. %) alloy all H atoms are trapped by Mo atoms and are located at sites displaced from  $T$  sites by about  $0.6 \text{ \AA}$  towards the Mo atoms at substitutional sites, and that at 373 K they are detrapped and enter  $T$  sites.

As described above, in the Nb-Mo(3 at. %)-H(5 at. %) alloy some fraction of H atoms are trapped by the Mo atoms and the rest are free of trapping. A trapping efficiency,  $f$ , the number of H atoms trapped by one Mo atom, was roughly estimated from comparison of the observed  $\alpha$ -angular profiles with calculated profiles. The calculated profiles were obtained by taking the weighted average of the  $\alpha$ -angular profiles for trapped H atoms and those for untrapped H atoms (at  $T$  sites) for a given trapping efficiency. As  $\alpha$ -angular profiles for

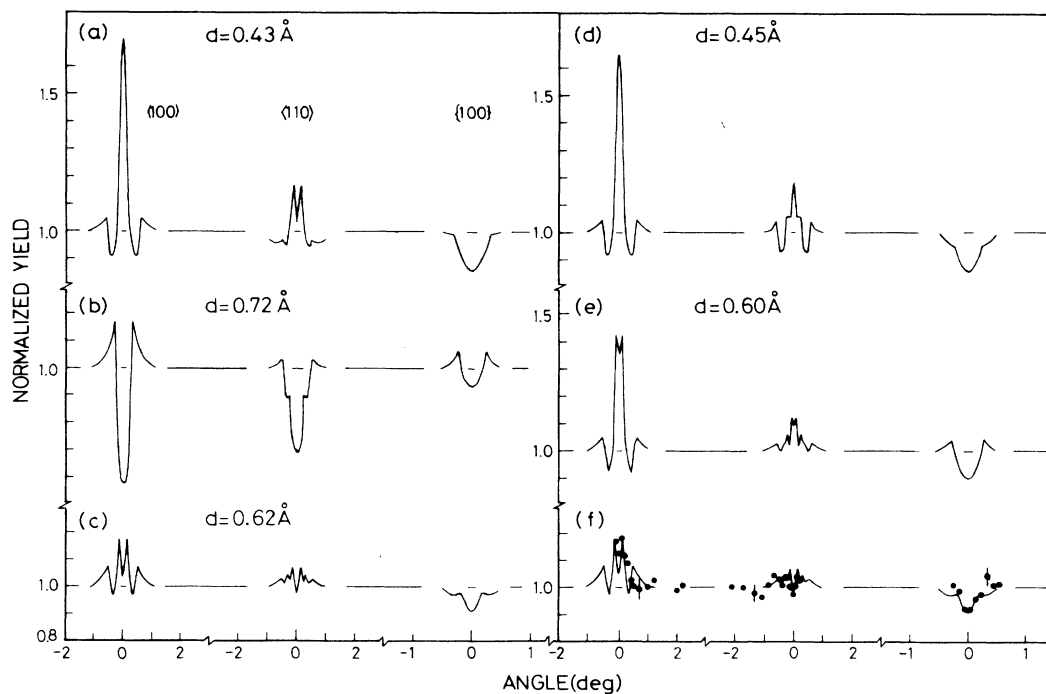


FIG. 4.  $\alpha$ -angular profiles calculated for various types of lattice location (a)–(e) in Fig. 3. (f) shows the comparison between observed  $\alpha$ -angular profiles for the Nb-Mo(3 at. %)-H(2 at. %) alloy and calculated profiles (solid curves) for the lattice location of type (c) in Fig. 3.

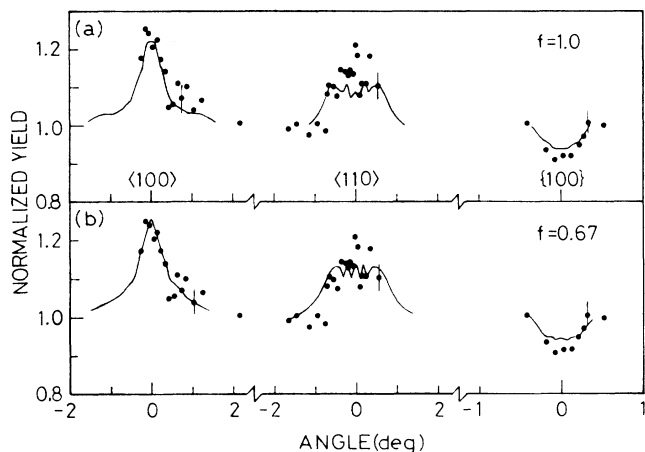


FIG. 5. Comparison between observed  $\alpha$ -angular profiles and calculated profiles (solid curves) for the Nb–Mo(3 at.%)–H(5 at.%) alloy for the trapping efficiency of (a)  $f = 1.0$  and (b)  $f = 0.67$ .

trapped H atoms, those obtained on the Nb–Mo(3 at.%)–H(2 at.%) alloy [Fig. 1(a)] were used. As for untrapped H atoms, the profile obtained on the Nb–Mo(3 at.%)–H(5 at.%) alloy for the  $\langle 100 \rangle$  channel at 373 K was used, together with those obtained on the Nb–H system for the  $\langle 110 \rangle$  and  $\{100\}$  channels (Fig. 1 in Ref. 16). Comparison between the observed profiles and calculated profiles for  $f = 0.67$  and 1.0 is shown in Fig. 5. For these values, the observed profiles are rather well reproduced,  $f = 0.67$  being slightly more favorable.

Hence, the trapping efficiency is roughly estimated to be 0.67–1.0 at room temperature in the Nb–Mo(3 at.%) alloy. This result is consistent with the estimate of Matsumoto *et al.* ( $f \approx 1.0$ ) from the H concentration dependence of a halfwidth of an x-ray reflection line in Nb–Mo(5 at.%) alloys<sup>1</sup> and a <sup>93</sup>Nb NMR absorption line in Nb–V[(5–8) at.%) alloys.<sup>3</sup> From these values of  $f$  the binding energy between hydrogen and Mo atoms was roughly estimated to be an order of 0.05 eV.

In conclusion, the present results give direct evidence for the existence of the attractive interaction between Mo atoms and hydrogen in Nb–Mo(3 at.%) alloys, and strongly support the trapping model for the mechanism of the enhancement of the TSH in Nb on alloying with Mo atoms, at least in the low concentration region of Mo solute atoms. At higher solute concentration, or in concentrated binary alloys, there will be a statistical distribution of local atomic configurations and concomitant distribution of interstitial-site energies. Accordingly, both the location of hydrogen and trapping behavior should become less well defined, and some description in terms of some average quantities would become more appropriate. We plan to extend the present work to higher-solute concentrations and other solute species.

The authors thank Mr. T. Urai for his technical assistance. Two of the authors (S.N. and F.K.) are grateful to Professor T. Osaka for his encouragement. This research was partially supported by the Ministry of Education, Science and Culture, Japan.

\*On leave from School of Science and Engineering, Waseda University, Shinjuku-ku, Tokyo 160, Japan.

<sup>1</sup>T. Matsumoto, Y. Sasaki, and M. Hihara, *J. Phys. Chem. Solids* **36**, 215 (1975).

<sup>2</sup>Y. Sasaki and M. Amano, in *Proceedings of the Second International Congress on Hydrogen in Metals, Paris, 1977*, edited by International Association for Hydrogen Energy (Pergamon, Oxford, 1977), p. 3C<sub>3</sub>.

<sup>3</sup>T. Matsumoto, *J. Phys. Soc. Jpn.* **42**, 1583 (1977).

<sup>4</sup>D. G. Westlake and J. F. Miller, *J. Less-Common Met.* **65**, 139 (1979).

<sup>5</sup>S. Tanaka and H. Kimura, *Trans. Jpn. Inst. Met.* **20**, 647 (1979).

<sup>6</sup>J. F. Miller and D. G. Westlake, in *Proceedings of the Second Japan Institute of Metals International Symposium on Hydrogen in Metals, Minakami, 1979* [*Trans. Jpn. Inst. Metals* **21**, Suppl., 153 (1980)].

<sup>7</sup>G. Cannelli, R. Cantelli, and M. Koiwa, *Philos. Mag. A* **46**, 483 (1982).

<sup>8</sup>R. Kirchheim, P. C. Camargo, and J. R. G. Da Silva, *J. Less-Common. Met.* **95**, 293 (1983).

<sup>9</sup>L. Lichty, J. Shinar, R. G. Barnes, D. R. Torgeson, and D. T. Peterson, *Phys. Rev. Lett.* **55**, 2895 (1985).

<sup>10</sup>D. T. Peterson and S. O. Nelson, *Metall. Trans.* **16A**, 367 (1985).

<sup>11</sup>D. T. Peterson and H. M. Herro, *Metall. Trans.* **17A**, 645 (1986).

<sup>12</sup>W. A. Oates and T. B. Flanagan, *Acta Metall.* **33**, 693 (1985).

<sup>13</sup>E. Yagi, T. Kobayashi, S. Nakamura, Y. Fukai, and K. Watanabe, *J. Phys. Soc. Jpn.* **52**, 3441 (1983).

<sup>14</sup>E. Yagi, T. Kobayashi, S. Nakamura, Y. Fukai, and K. Watanabe, *Phys. Rev. B* **31**, 1640 (1985).

<sup>15</sup>E. Yagi, T. Kobayashi, S. Nakamura, F. Kano, K. Watanabe, Y. Fukai, and S. Koike, *Phys. Rev. B* **33**, 5121 (1986).

<sup>16</sup>E. Yagi, S. Nakamura, T. Kobayashi, K. Watanabe, and Y. Fukai, *J. Phys. Soc. Jpn.* **54**, 1855 (1985).

<sup>17</sup>C. Erginsoy, *Phys. Rev. Lett.* **15**, 360 (1965).

<sup>18</sup>D. Van Vliet, *Radiat. Eff.* **10**, 137 (1971).